Instability of a domain wall in electric current: Role of topological charge

E. A. Karashtin* and A. A. Fraerman
Institute for Physics of Microstructures RAS, GSP-105, Nizhny Novgorod 603950, Russia
and University of Nizhni Novgorod, 23 Prospekt Gagarina, Nizhny Novgorod 603950, Russia
(Received 26 January 2015; revised manuscript received 24 April 2015; published 6 July 2015)

We theoretically show that the electric current applied in the plane of a Bloch domain wall introduces a mechanism of its stability or instability that is strongly connected to its topological charge. In the case of a wall in an infinite ferromagnet, applying a current in one direction leads to the instability, while a current in the opposite direction the wall is stable. This property is caused by the toroidal moment of the system and appears to be due to the magnetostatic energy of the domain wall. A more complicated case of a ferromagnetic slab is considered.

DOI: 10.1103/PhysRevB.92.014401 PACS number(s): 75.70.Kw, 75.78.Fg, 72.25.Ba, 75.30.Ds

I. INTRODUCTION

The influence of an electric current on the magnetic state of natural or artificial ferromagnets attracts a lot of attention [1–9]. Indeed, the possibility to change the magnetization of a ferromagnetic layer in a tunnel junction by applying an electric current is very promising for practical use, such as in creating magnetic memory [10]. The magnetic moment manipulation by electric current is used in different prototypes of magnetoresistive random access memory [11,12] and logic devices [13,14]. The phenomenon exploited here is called the spin torque effect [1,2]. The development of these new devices requires the investigation of domain-wall dynamics in electric current in artificial structures such as a ferromagnetic wire [13] and under the influence of additional parameters (e.g., the Dzyaloshinskii-Moriya interaction strongly affects the domain-wall motion and structure [15]).

In the simplest way, if we take a Bloch domain wall in a ferromagnet with the "easy axis" anisotropy and apply the electric current perpendicular to its surface, the wall will move [7,9]. However, the behavior of such a wall if the electric current is applied in its plane needs additional investigation. It is well known that a domain wall in an infinite ferromagnet remains stable due to the surface tension [16,17], while in a slab the magnetostatic energy at the surfaces appears and the wall becomes unstable [18]. In this paper we show that an electric current applied in the plane of the domain wall introduces a new mechanism of its stability or instability that is strongly connected to its topological charge [19].

In Sec. II we write out general assumptions and describe a mathematical approach to the highlighted problem. Section III is devoted to the results for a domain wall in an infinite ferromagnet and in a ferromagnetic slab. We show that total stability or instability of a domain wall is determined by the concurrency of three mechanisms related to the surface tension, to the magnetostatic energy at the slab interfaces, and to the electric current. The latter strongly depends on direction of the toroidal moment of the system with respect to the electric current vector. Discussion and estimations for typical parameters of Co ferromagnet (that is supposed to be magnetized perpendicularly to the slab plane) are collected in Sec. IV. A summary of our results is outlined in Sec. V. The Appendix contains calculation details.

II. THE EQUATIONS AND MAIN ASSUMPTIONS

We start from the Landau-Lifshitz-Gilbert (LLG) equation [4] in the form

$$\frac{\partial \mathbf{M}}{\partial t} = -\gamma[\mathbf{M}\times\mathbf{H}_{\text{eff}}] + \alpha\left[\mathbf{M}\times\frac{\partial \mathbf{M}}{\partial t}\right] + b(\mathbf{j}\cdot\nabla)\mathbf{M} - c[\mathbf{M}\times(\mathbf{j}\cdot\nabla)\mathbf{M}], \quad (1)$$

where $\mathbf{M}$ is the magnetization vector normalized by M_s (thus being a unit vector), $\mathbf{j}$ is the density of applied electric current, $\mathbf{H}_{\text{eff}} = \mathbf{H} - \frac{\delta w}{\delta \mathbf{M}}$ is the effective magnetic field vector (w is the energy density functional), $\mathbf{H}_{\text{eff}}$ is in the units of the saturation magnetization M_s here, while w is normalized by M_s^2. All the constants γ, α, b, c in (1) are positive; b describes the adiabatic contribution of the current, while c determines the nonadiabatic one [4]. $\mathbf{H}$ in the definition of $\mathbf{H}_{\text{eff}}$ is a "true" magnetic field that is bound to the magnetic moment $\mathbf{M}$ via the Maxwell equations:

$$\text{rot}\mathbf{H} = 0; \quad \text{div}(\mathbf{H} + 4\pi\mathbf{M}) = 0. \quad (2)$$

Note that we have excluded the magnetostatic energy associated with $\mathbf{H}$ from the energy density w for the sake of convenience, adding $\mathbf{H}$ to $\mathbf{H}_{\text{eff}}$ directly instead.

The considered system is depicted in Fig. 1. The magnetization is supposed to have the form

$$\mathbf{M} = (n\sin\theta\cos\phi, n\sin\theta\sin\phi, m\cos\theta) \quad (3)$$

in the Cartesian coordinate system where the y axis is perpendicular to the domain wall and the x axis parallel to it, as shown in Fig. 1. The n and m constants in (3) take the ±1 values; the former determines the direction of magnetization rotation in the domain wall (domain-wall chirality), and the latter stands for the direction of the toroidal moment [20] $\mathbf{T} = \frac{1}{V}\int[\mathbf{r}\times\mathbf{M}]dV = (T_x,0,0)$ of the system: $m = 1$ corresponds to $T_x < 0$; $m = -1$ corresponds to $T_x > 0$. In an unperturbed domain wall, $\phi = \phi_0 = 0$, while $\theta = \theta_0$ is determined as

$$\theta_0 = 2\arctan[\exp(y/\Delta)], \quad (4)$$

where Δ is the domain-wall thickness. We add a small perturbation to the shape of the domain wall as follows (the

*eugenk@ipmras.ru

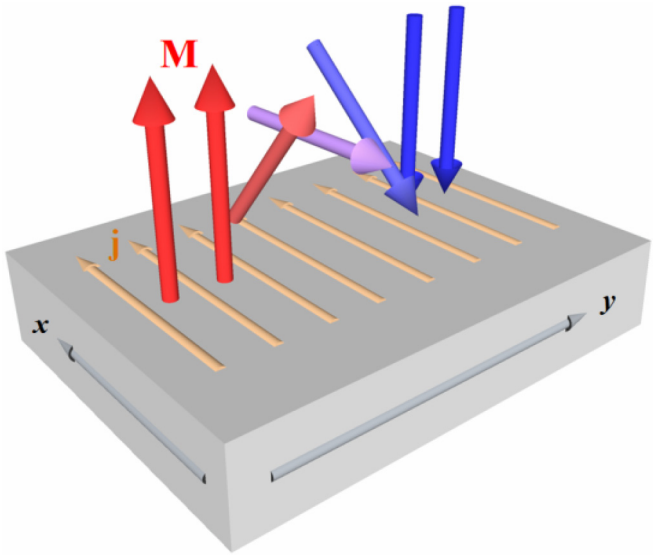

FIG. 1. (Color online) The geometry of the system.

Slonczewski parametrization [17]):

$$\phi = \phi(x,t); \quad \theta = 2\arctan\left\{\exp\left[\frac{y - q(x,t)}{\Delta}\right]\right\}. \tag{5}$$

An electric current flows in the direction of the x axis, being parallel to the unperturbed domain-wall plane.

In order to find ϕ and q, we write the energy density supposing "easy axis" anisotropy of a ferromagnet [16],

$$w = \lambda[(\nabla\theta)^2 + \sin^2\theta(\nabla\phi)^2] - K\cos^2\theta, \tag{6}$$

where λ is the exchange constant (it is normalized by M_s^2 and has the dimension cm^2 in our parametrization) and K is the anisotropy constant. The domain-wall thickness Δ may be defined via these constants as $\Delta = \sqrt{\lambda/K}$. First, two terms of the right-hand side of (6) are often interpreted as the surface tension energy density [16,17] after integrating over the y coordinate that is perpendicular to the domain wall.

Restricting ourselves to the linear in ϕ and q approximation, we find $\mathbf{H}(k_x,y,z)$ from (2), where k_x is the x component of the wave vector; the magnetic field is thus small (linear in ϕ and q), excluding the zero-order part of the z component associated with the edges of the slab that obviously exists for a straight domain wall. In order to simplify the equations, we also average $\mathbf{H}$ over the z coordinate. Indeed, we are not interested in the nonuniform solution of (1) that may appear only due to the dependence of the magnetic field $\mathbf{H}$ on the z coordinate and is important for a thick slab. Since ϕ and q do not depend on the y coordinate perpendicular to the wall, we may also integrate Eq. (1) over it. Next, we apply the Fourier transform over the x coordinate and over t to (1), introducing the frequency ω. After simplification, we get a system of two linear equations for $\tilde{q}(k_x,\omega) = \int q(x,t)\exp(ik_x x - i\omega t)dxdt$ and $\tilde{p}(k_x,\omega) = \tilde{\phi}(k_x,\omega)\Delta = \int \phi(x,t)\exp(ik_x x - i\omega t)dxdt\Delta$ that describes the behavior of the system. Further details regarding these equations are found in the Appendix.

In next sections we analyze the growth rate (i.e., the imaginary part of frequency ω) depending on the wave vector k_x for different parameters of the system. It could be calculated by placing a condition that the system of Eqs. (A1) and (A2) has a nontrivial solution. A positive sign of the growth rate means that the system is unstable with respect to the perturbation of the selected wave vector k_x and frequency ω associated with it. We find the parameter region of system instability for the case of an infinite ferromagnet and a ferromagnetic slab.

III. THE CONDITION OF DOMAIN-WALL INSTABILITY

A. Infinite ferromagnet

First of all, let us analyze the case when the slab thickness is infinite ($d \to \infty$). In this case we find the dispersion law and get the condition of positive imaginary part of ω,

$$k_x^2\left[\frac{1}{2\pi}l_j^2 - (\lambda_1+\lambda_2)\Delta m l_j - 2\alpha l_{ex}^2\left(\lambda_1 + k_x^2\Delta^2\lambda_2 + \frac{k_x^2 l_{ex}^2}{\pi}\right)\right] > 0, \tag{7}$$

where $\lambda_1,\lambda_2,\lambda_3$ are the integrals defined by (A3). Here we introduced the length associated with the electric current,

$$l_j = \frac{\alpha b - c}{\gamma} j_x, \tag{8}$$

that, however, may change its sign when the component j_x changes sign. Its physical meaning is related to spin transfer by electric current. Besides, the exchange length [16] usually written as $\sqrt{\lambda/M_s^2}$ up to a constant multiplier takes the form $l_{ex} = \sqrt{\lambda}$ in our parametrization. We see from (7) that the growth rate tends to zero when $k_x \to 0$. Next, we should note that if there is no electric current the condition (7) is never satisfied. Indeed, the integrals λ_1 and λ_2 are not negative. Taking $l_j = 0$, we see that the left-hand side of (7) is less than or equal to zero for all k_x. This is consistent with the well-known fact that a domain wall is stable in an infinite ferromagnet due to the surface tension.

Application of a large electric current of any sign leads to the instability of the system due to the first term in the left-hand side of (7) that is proportional to l_j^2. However, for all known materials the b and c constants are very small [4,5]; hence, l_j is very small, too, compared to other length scales for the realistic values of current (up to $10^8 A/\mathrm{cm}^2$). So we may neglect the term proportional to l_j^2 with good accuracy.

The second term in the left-hand side of (7) appears to be due to the magnetostatic energy and is linear in l_j and in the toroidal moment of the system. If $ml_j > 0$, this term contributes to the stability of the system, while for $ml_j < 0$ it may lead to its instability, depending on the k_x value. For small k_x ($k_x \ll 1/\Delta$) we use approximate calculations of $\lambda_1,\lambda_2,\lambda_3$ (A7) and (7) and get a simple condition of instability:

$$|k_x| m l_j + 2\alpha l_{ex}^2 k_x^2 < 0. \tag{9}$$

The first term in the left-hand side of (9) tends to zero slower than the second one as $k_x \to 0$. Hence, even a very small electric current causes the domain-wall instability for small-enough values of $|k_x|$.

The sign of ml_j is determined by the direction of the electric current with respect to the vector of the toroidal moment and by the sign of the constant $(\alpha b - c)$. Although $c \ll b$ and $\alpha \ll 1$, we suppose, for the sake of simplicity, that this constant is positive. Taking this speculation into account, the electric current applied to the domain wall in an infinite ferromagnet leads to its instability if it is parallel to the toroidal moment of the system. If the current is antiparallel to the toroidal moment, it adds to the stability of the domain wall.

B. Ferromagnetic slab

In the case of a ferromagnetic slab we should add the magnetostatic energy that appears due to the edges of the slab. This leads to additional terms in the condition for domain-wall instability (7):

$$k_x^2\left[\frac{1}{2\pi}l_j^2-(\lambda_1+\lambda_2)\Delta m l_j-2\alpha l_{ex}^2\left(\lambda_1+k_x^2\Delta^2\lambda_2+\frac{k_x^2l_{ex}^2}{\pi}\right)\right] - 4\alpha\left(\lambda_1+\frac{k_x^2l_{ex}^2}{\pi}\right)[\lambda_3(k_x)-\lambda_3(0)]\frac{\Delta}{d}>0. \quad (10)$$

As earlier, the condition depends on ml_j and does not depend on n. So the chirality of the domain wall does not affect its stability or instability, while the toroidal moment exerts influence on it only together with the electric current.

It can be shown that $\lambda_3(k_x) < \lambda_3(0)$ for nonzero k_x. Thus, the additional term in (10) contributes to the instability of the domain wall. In the absence of an electric current domain-wall stability is determined by the concurrence between the magnetostatic energy that appears due to the z component of the magnetic field and the surface tension. Using the approximations (A7) we get

$$2\frac{\Delta}{d}[\Gamma + K_0(2|k_x|d) + \ln(|k_x|d)] - k_x^2l_{ex}^2 > 0, \quad (11)$$

which corresponds to known results [18]. According to this condition, the domain wall is unstable for small k_x (excluding $k_x = 0$), while for large k_x it becomes stable. In order to visualize this result, one may use approximations for the modified Bessel function $K_0(2|k_x|d) \approx -[\Gamma + \ln(|k_x|d)](1 + |k_x|^2d^2) + |k_x|^2d^2$ for $|k_x|d \ll 1$ and $K_0(2|k_x|d) \approx \frac{\exp(-2|k_x|d)}{\sqrt{2|k_x|d}}$ for $|k_x|d \gg 1$ [21].

The addition of an electric current modifies (11) to

$$4\alpha\frac{\Delta}{d}[\Gamma + K_0(2|k_x|d) + \ln(|k_x|d)] - 2\alpha k_x^2l_{ex}^2 - |k_x|ml_j > 0, \quad (12)$$

where we used the approximation (A7) again. We see from (12) that if the electric current is parallel to the toroidal moment of the system it adds to the instability of the domain wall, while if it is antiparallel to the toroidal moment it contributes to the stability of the wall (e.g., for small $|k_x|$ the wall becomes stable) and may, in theory, lead to its stability for all k_x. However, in practice it just slightly changes the range of values of k_x where the domain wall is unstable due to the very small constants b and c that determine the influence of the current, as discussed in Sec. IV.

IV. DISCUSSION

The new mechanism of domain-wall stability or instability may be qualitatively understood in the following way. The magnetization distribution in a plane domain wall has two components: M_x and M_z. If we perturb the domain wall and take into account only its surface tension it still has two components (neglecting magnetization precession). Adding the magnetostatic energy leads to local turn of magnetization of the domain wall to the direction tangential to its surface. Thus, all three components of the magnetization are nonzero, which, in turn, leads to the appearance of *topological charge* [19,22] $Q \sim (\mathbf{M}\cdot[\frac{d\mathbf{M}}{dx}\times\frac{d\mathbf{M}}{dy}])$, which has the form $Q \sim -2m\phi_x'$ for the magnetization distribution described by (3)–(5). In the considered case the topological charge has different sign for areas with different directions of deviation from initial plane (see Fig. 2). We may further associate this topological charge to small pieces of virtual skyrmions. If a current is applied to the system the skyrmions will move [22]; we are interested in the component of their velocity that is perpendicular to the domain wall. The direction of this component does not depend on the chirality of domain wall (i.e., on the n constant), but depends on the direction of skyrmion core (i.e., on the m constant) and on the direction of current [compare Figs. 2(a) and 2(b)]. For one direction of current virtual skyrmions move away from each other; so do the topological charges of domain-wall areas, and the perturbation of the domain wall becomes smaller, which leads to its stability [Fig. 2(a)]. For another direction of current the direction of perpendicular movement is opposite and the perturbation increases [Fig. 2(b)].

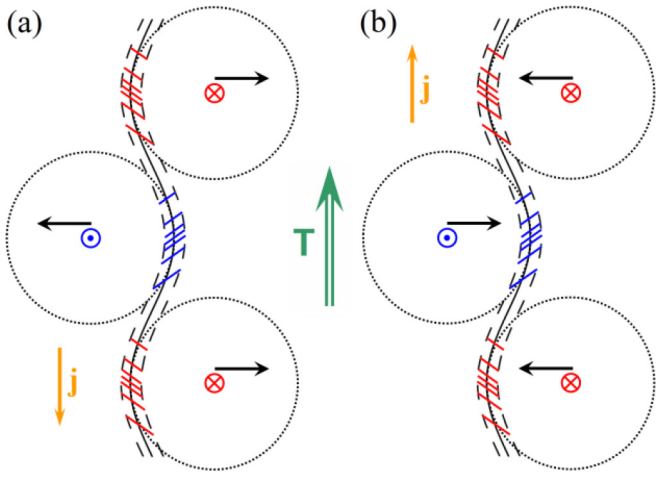

FIG. 2. (Color online) The mechanism of (a) domain-wall stability and (b) domain-wall instability in electric current. The solid line stands for the domain wall; dashed lines show its range. Areas of the domain wall that have topological charge of different sign are hatched in different directions (red and blue online); the density of hatches corresponds to the magnitude of the charge. Dotted lines show virtual skyrmions that approximate parts of the domain wall. Arrows show the perpendicular movement when the current is applied.

As has been mentioned, our results agree to the known results for domain-wall stability without the electric current. In order to analyze these results, we may further find the typical length scale of appearing deviations. For rough estimations, we may suppose that this scale corresponds to the maximum of the growth rate since the deviation of this scale rises faster than of any other. For an infinite ferromagnet we get the absolute value of k_x^* under approximations (A7),

$$k_x^* = -\frac{1}{4\alpha l_{ex}}\frac{m l_j}{l_{ex}}, \tag{13}$$

where we suppose that for negative k_x^* there is no instability, and for a slab we arrive at

$$k_x^* = \frac{1}{d}\exp\left(\frac{1-2\Gamma}{2}\right)\exp\left(-\frac{l_{ex}^2}{2d\Delta}\right) - \frac{m l_j}{8\alpha d\Delta}, \tag{14}$$

supposing that the electric current adds a small correction to the scale. The first term in the right-hand side of (14), again, corresponds to known results without the electric current [23,24], while the second term is a small correction driven by the current. Importantly, the conditions of instability (7) and (10) are even with k_x, which means that the waves running in both directions of x have the same growth rate. The formula (14) works for $d \gg l_{ex}$ when the second term in its right-hand side is much smaller than the first one. However, we see that for small d ($d \ll l_{ex}$) the first term decreases exponentially, while the second one increases as $1/d$. For ultrathin layers ($d \to 0$) and appropriate sign of current the typical scale k_x^* tends to the value determined by (13).

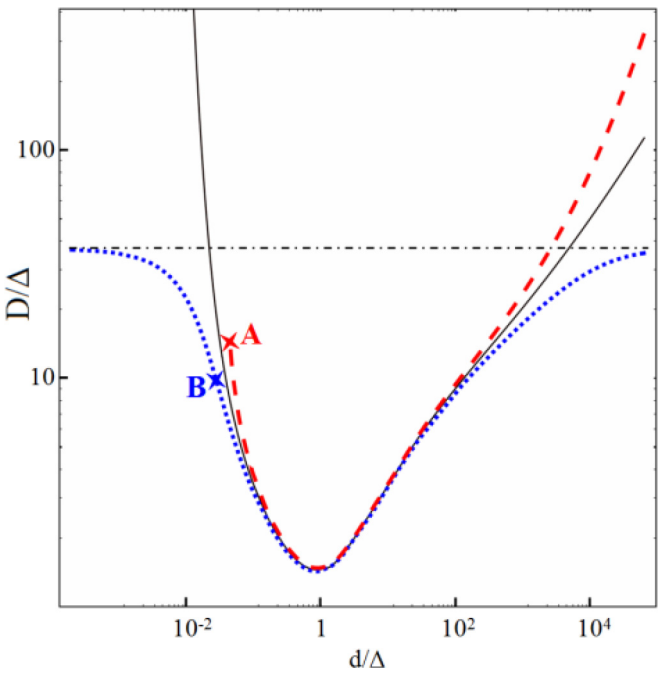

FIG. 3. (Color online) Dependence of typical length scale $D = 1/k^*$ on the layer half thickness d. The solid (black) line stands for zero current; dashed (red) and dotted (blue) lines correspond to $j_x = 10^8$ A/cm^2 and $j_x = -10^8$ A/cm^2. The dot-dashed line determines the asymptote defined by (13). The A point on the dashed (red) line is the point where the domain wall becomes stable due to the applied current. The B point on the dotted (blue) line corresponds to the d/Δ value at which D is two times smaller if the current is applied than that without the current.

The perpendicular-to-plane magnetization is observed in Co/Pt multilayer structures [25,26], including the case of one Co layer. We perform estimations for the parameters of Co ferromagnet: $M_s = 1446$Oe, $\gamma = 2.7\times10^{10}$ s^{-1}, $\alpha = 0.1$, $b = 1.4\times10^{-5}\frac{cm^3}{A\cdot s}$, $c = 2.8\times10^{-7}\frac{cm^3}{A\cdot s}$, $\Delta = 24.3$ nm, $l_{ex} = 9.8$ nm [4,5]. The electric current affects the region of domain-wall instability and the maximum of the growth rate. The calculation of typical length scale $D = 1/k_x^*$ versus d for ultrathin layers is represented in Fig. 3. We see that the influence of current is essential for ultrathin layers with $d/\Delta \ll 1$: Applying current of one direction leads to stability of the domain wall (for d less than d of the A point in Fig. 3). For another direction of current the scale of instability differs from the value obtained in the absence of current (for instance, the scale is two times smaller than that without the current for $d/\Delta \approx 0.028$; see point B in Fig. 3).

V. CONCLUSION

We have theoretically studied stability of a Bloch domain wall in the presence of electric current applied in its plane. The resulting stability or instability of a domain wall is determined by the concurrency of three mechanisms: The surface tension leads to the domain-wall stability in the case of an infinite ferromagnet, the magnetostatic energy at the interfaces of the slab makes the domain wall unstable, and the electric current may either contribute to the stability or instability, depending on its direction with respect to the vector of system toroidal moment. According to our calculations, in the case of a wall in an infinite ferromagnet applying a current in one direction leads to an addition to the stability of the wall while for the opposite direction of the current it becomes unstable. In the case of a ferromagnetic slab the electric current leads to a correction to the wavelength range of the domain-wall instability and to the typical length size of inhomogeneity, which seems to be essential in ultrathin layers.

In conclusion, we have shown that the electric current applied in the plane of the domain wall reveals a new mechanism of its stability or instability. Although we considered only the case of small deviations of the domain-wall shape, we suppose that the size of domains in the resulting domain structure would change if a current is applied, which may further allow to control the domain structure of thin ferromagnetic films.

ACKNOWLEDGMENTS

The authors are grateful to M. V. Sapozhnikov for stimulating discussions. The research is partly supported by a grant of The Ministry of Education (the agreement of August 27, 2013 No. 02.B.49.21.0003), and by RFBR Grant No. 14-02-00448.

APPENDIX: THE EQUATIONS OF DOMAIN-WALL MOTION

We apply the approach described in Sec. II to the LLG equation (1) with the magnetization **M** defined by (3) and (5). We get the following equations for the Fourier transform of the phase $\phi\Delta = p$ and thedomain-wall shift q:

$$[\omega + j_x k_x b - 2\pi\gamma\Delta k_x \lambda_1(k_x) m]\tilde{q} - \{\alpha\omega + j_x k_x c + i2\gamma[\lambda k_x^2 + \pi\lambda_1(k_x)]\}\tilde{p}m = 0; \tag{A1}$$

$$[\omega + j_x k_x b - 2\pi\gamma\Delta k_x \lambda_2(k_x) m]\tilde{p}m + \left(\alpha\omega + j_x k_x c + i2\gamma\left\{\lambda k_x^2 + \pi\Delta^2 k_x^2 \lambda_2(k_x) + 2\frac{\Delta}{d}[\lambda_3(k_x) - \lambda_3(0)]\right\}\right)\tilde{q} = 0; \tag{A2}$$

$$\lambda_1(k_x) = 2\int_0^\infty \frac{v^2}{\left(v^2 + \pi^2\Delta^2 k_x^2/4\right)\cosh^2 v} dv; \quad \lambda_2(k_x) = 2\int_0^\infty \frac{v}{\left(v^2 + \pi^2\Delta^2 k_x^2/4\right)\sinh v \cosh v} dv;$$

$$\lambda_3(k_x) = \int_0^\infty \frac{v\left[1 - \exp\left(-\frac{2d}{\pi\Delta}\sqrt{v^2 + \pi^2\Delta^2 k_x^2/4}\right)\right]}{\sinh v \cosh v\sqrt{v^2 + \pi^2\Delta^2 k_x^2/4}} dv. \tag{A3}$$

The integrals $\lambda_{1,2,3}(k_x)$ in (A1) and (A2) that arise from the magnetostatic energy of the wall are written out in (A3) and could not be taken exactly. However, the domain-wall thickness Δ is typically very small (10–20 nm) and in order to simplify the equations we may consider the case of a quite thick slab and suppose that the deviation of the wall also has quite big wavelength:

$$\Delta \ll d, \tag{A4}$$

$$k_x\Delta \ll 1. \tag{A5}$$

The integral λ_3 appears at the edges of the slab and characterizes the magnetostatic energy due to nonzero z component of magnetic field. In order to simplify this integral, we put a stronger restriction on k_x,

$$k_x d \ll 1, \tag{A6}$$

which means we consider the deviations of the scale that is much bigger than the slab thickness. Taking into account (A4)–(A6), we obtain

$$\lambda_1 \approx 2, \quad \lambda_2 \approx \frac{2}{\Delta|k_x|}, \quad \lambda_3(k_x) - \lambda_3(0) \approx -[\Gamma + K_0(2|k_x|d) + \ln(|k_x|d)], \tag{A7}$$

where $\Gamma \approx 0.5772$ is the Euler constant and K_0 is the Macdonald function [21]. Numeric calculations show that the approximations (A7) may be used for small k_x.

[1] J. C. Slonczewski, J. Magn. Magn. Mater. **159**, L1 (1996).
[2] L. Berger, Phys. Rev. B **54**, 9353 (1996).
[3] Y. B. Bazaliy, B. A. Jones, and S.-C. Zhang, Phys. Rev. B **57**, R3213 (1998).
[4] S. Zhang and Z. Li, Phys. Rev. Lett. **93**, 127204 (2004).
[5] Z. Li and S. Zhang, Phys. Rev. B **70**, 024417 (2004).
[6] A. V. Khvalkovskiy, K. A. Zvezdin, Ya. V. Gorbunov, V. Cros, J. Grollier, A. Fert, and A. K. Zvezdin, Phys. Rev. Lett. **102**, 067206 (2009).
[7] J. Lindner, Superlattices Microstruct. **47**, 497 (2010).
[8] O. Boulle, G. Malinowski, and M. Kläui, Mater. Sci. Eng., R **72**, 159 (2011).
[9] J. Shibata, G. Tatara, and H. Kohno, J. Phys. D: Appl. Phys. **44**, 384004 (2011).
[10] J. A. Katine and E. E. Fullerton, J. Magn. Magn. Mater. **320**, 1217 (2008).
[11] S. S. P. Parkin, M. Hayashi, and L. Thomas, Science **320**, 190 (2008).
[12] D. Atkinson, D. S. Eastwood, and L. K. Bogart, Appl. Phys. Lett. **92**, 022510 (2008).
[13] D. A. Allwood, G. Xiong, C. C. Faulkner, D. Atkinson, D. Petit, and R. P. Cowburn, Science **309**, 1688 (2005).
[14] V. L. Mironov, O. L. Ermolaeva, E. V. Skorohodov, and A. Y. Klimov, Phys. Rev. B **85**, 144418 (2012).
[15] O. A. Tretiakov and A. Abanov, Phys. Rev. Lett. **105**, 157201 (2010).
[16] L. D. Landau and E. M. Lifshitz, *Course of Theoretical Physics: Electrodynamics of Continuous Media* (Butterworth-Heinemann, Oxford, UK, 1984), Vol. 8.
[17] A. P. Malozemoff and J. C. Slonczewski, *Magnetic Domain Walls in Bubble Materials* (Academic Press, New York, London, 1979).
[18] F. B. Hagedorn, J. Appl. Phys. **41**, 1161 (1970).
[19] A. M. Kosevich, B. A. Ivanov, and A. S. Kovalev, Phys. Rep. **194**, 117 (1990).
[20] V. M. Dubovik and V. V. Tugushev, Phys. Rep. **187**, 145 (1990).
[21] J. Spanier and K. B. Oldham, *An Atlas of Functions* (Hemisphere, Washington, 1987).
[22] A. Thiele, Phys. Rev. B **7**, 391 (1973).
[23] D. Stickler, R. Frömter, H. Stillrich, C. Menk, H. P. Oepen, C. Gutt, S. Streit-Nierobisch, Lorenz-M. Stadler, G. Grübel, C. Tieg, and F. Yakhou-Harris, Phys. Rev. B **84**, 104412 (2011).
[24] B. Kaplan and G. A. Gehring, J. Magn. Magn. Mater. **128**, 111 (1993).
[25] Y. Ochiai, S. Hashimoto, and K. Aso, IEEE Trans. Magn. **25**, 3755 (1989).
[26] P. F. Carcia and W. B. Zeper, IEEE Trans. Magn. **26**, 1703 (1990).